

The numerical solution of the problem of linear compression of a viscous, porous material in a cylindrical die is used as a basis for describing the regular, wave, and transient compaction conditions. The standard conditions for the operation of different compaction modes are determined.

Introduction. It is known that qualitatively different compaction conditions, the regular [1-3] and the wave [4] mode, can occur in compacting hot powder materials. The regular compaction mode involves instantaneous transmission of the perturbation from the plunger to the entire volume of the material to be compacted, while the inertia of the medium is virtually absent ($Re \ll 1$) [3]. The wave compaction mode occurs when the perturbations are transmitted successively from the plunger, and compaction is localized in a narrow compression zone. Such conditions are characterized by rather large Re numbers [4].

Theoretical investigations of the wave and the regular compaction modes do not provide an answer to the question concerning the standard conditions of their occurrence. Taking into account the limiting nature of both sets of conditions, it is important to consider the many variants of conditions of compacting a porous powder mass, brought to a high temperature. This also involves investigation of the transient processes occurring in the intermediate range of Reynolds numbers. The mathematical description of the regular and the wave modes given in [1-4] is based on the steady-state equations of motion. However, calculations of the transient characteristics of the compaction process and the dynamics of speed and density variation throughout the volume of the material to be compacted are of practical importance. These problems can be solved on the basis of a generalized model by means of numerical investigations of nonstationary equations of continuity and motion, simultaneously with rheological relationships.

Statement of the Problem. We shall consider here axial, linear compression of a hot powder material in a cylindrical die. The behavior of the material in compaction is described by the following system of equations of continuity,

$$\frac{\partial \rho}{\partial t} + \frac{\partial}{\partial x} (\rho u) = 0 \quad (1)$$

and motion,

$$\rho \rho_1 \left(\frac{\partial u}{\partial t} + u \frac{\partial u}{\partial x} \right) = \frac{\partial \sigma}{\partial x} \quad (2)$$

simultaneously with the rheological relationship

$$\sigma = \frac{4}{3} \eta_1 \frac{\rho^m}{1 - \rho} \frac{\partial u}{\partial x} \quad (3)$$

The density (porosity) distribution along the pressing height is assigned at the initial instant of time:

Institute of Structural Macrokinetics, Academy of Sciences of the USSR, Chernogolovka.
Translated from *Inzhenerno-Fizicheskii Zhurnal*, Vol. 62, No. 3, pp. 411-415, March, 1992.
Original article submitted July 16, 1991.

$$\rho|_{t=0} = \rho_0(x). \quad (4)$$

We assume that material flow is absent at the lower boundary of the specimen,

$$u|_{x=0} = 0, \quad (5)$$

while, at the upper end of the specimen, there occurs either operation at the assigned pressing rate,

$$u|_{x=H(t)} = -u_p(t),$$

or operation with the assigned pressing force,

$$p|_{x=H(t)} = -N_p(t), \quad (6)$$

which is considered below.

It should be noted that the statement of problem (1)-(6) comprises the equation of motion comprising the transient and inertial terms, which makes it possible to consider various transient processes in compaction: operation where the regular or the wave mode is established, describe the range with respect to the Re number between these two limiting cases of compaction, etc.

The Lagrange coordinates were used in [3, 5] for solving problems of uniaxial compression of visous, porous materials. Substituting the Lagrange variables q and τ for the x and t coordinates (the physical meaning of the Lagrange coordinates used here has been described in [3]), we arrive at the following system of equations:

$$\begin{aligned} \frac{\partial v}{\partial \tau} &= \frac{\partial u}{\partial q}, \\ \rho_1 \frac{\partial u}{\partial \tau} &= \frac{\partial \sigma}{\partial q}, \\ \sigma &= \frac{4}{3} \eta_1 \frac{1}{(v-1)v^m} \frac{\partial u}{\partial q}. \end{aligned} \quad (7)$$

The initial and the boundary conditions in the new coordinate system are the following:

$$\begin{aligned} \rho|_{\tau=0} &= \rho_0(q), \\ u|_{q=0} &= 0 \quad p|_{q=M(t)} = -N_p(t). \end{aligned}$$

The difference scheme of second-order accuracy is used for the numerical solution of the system of equations (7). Assume that Δq is the spatial step, while $\Delta \tau$ is the time step.

At the first step, the predictor, approximation of the specific volume \hat{v}_j^{n+1} with first-order accuracy with respect to time is realized:

$$\hat{v}_j^{n+1} = v_j^n + \frac{\lambda}{2} (u_{j+1}^n - u_{j-1}^n)$$

for $j \neq 0, N$

$$(u_j^n = u(j\Delta q, i\Delta \tau), 0 \leq j \leq N),$$

at the left-hand boundary,

$$\hat{v}_0^{n+1} = v_0^n + \lambda \left(2u_1 - \frac{1}{2} u_2 \right),$$

at the right-hand boundary,

$$\hat{v}_N^{n+1} = v_N^n - \Delta\tau \frac{3}{4} \frac{N_p}{\eta_1} \frac{1}{\mu_N^n},$$

where

$$\lambda = \Delta\tau/\Delta q, \quad \mu(v) = \frac{1}{(v-1)v^n}.$$

The second step — the velocity corrector — constitutes the analog of the Krant-Nicholson scheme:

for $j = 0, N$,

$$\begin{aligned} u_j^{n+1} = & u_j^n + \frac{\Delta\tau}{2\Delta q^2} \frac{4}{3} \frac{\eta_1}{\rho_1} \{ \hat{\mu}_{j+\frac{1}{2}}^n (u_{j+1}^n - u_j^n) - \\ & - \hat{\mu}_{j-\frac{1}{2}}^n (u_j^n - u_{j-1}^n) + \hat{\mu}_{j+\frac{1}{2}}^{n+1} (u_{j+1}^{n+1} - u_j^{n+1}) - \\ & - \hat{\mu}_{j-\frac{1}{2}}^{n+1} (u_j^{n+1} - u_{j-1}^{n+1}) \}. \end{aligned}$$

The trial-and-error method is used to solve the derived system of implicit equations with respect to the speed at the top layer u_j^{n+1} . Calculations performed by means of the above difference scheme have not revealed stability limitations.

Analysis of the Numerical Calculations Results: As a result of the numerical solution, we determined the density, speed, and stress fields in the volume of the material to be compacted. An analysis of the results of numerical experiments made it possible to determine the standard conditions for realizing different modes of compacting a hot, porous mass. The generalized Re number, an expression for which was obtained in [4], we chosen as the criterion determining whether a particular compaction mode is in operation:

$$\text{Re}(N) = \frac{\sqrt{N_p(1-\rho)/\rho_1\rho_2}}{\eta_1} \rho_1 H_0. \quad (8)$$

This is in fact a dimensionless set, which depends on the rheological and physical characteristics of the material to be compacted, the dimensions of the billet, and the technological parameters of the process. It is more convenient for analyzing the material flow for the assigned press force. The ranges of the Re number corresponding to the compaction modes described earlier [1-4] have been determined.

It has been found that one of the limiting cases occurs in the $\text{Re} < \text{Re}_*$ range: the regular compaction mode corresponding to a linear velocity profile and simultaneous compaction of all individual volumes within the hot, porous billet (Fig. 1a). The boundary value Re_* can be determined in analyzing the velocity and density profiles. It is clear that this boundary is rather relative, corresponding to $\text{Re}_* \sim 1$. The formation of a linear velocity profile does not occur instantaneously, but within the hydrodynamic stabilization time $\tau_h = H_0^2 \rho_1 / \eta_1$ (Fig. 1b). Numerical calculations make it possible to determine the time τ during which the effect of inertia on the compaction process manifests itself. For instance, for $\eta_1 = 10^6$ Pa·sec, $H_0 = 0.1$ m, $\rho_1 = 5 \cdot 10^3$ kg/m³, and $N_p = 10^9$ Pa ($\text{Re} = 0.2$), the hydrodynamic stabilization time is equal to $\tau_h = 5 \cdot 10^{-5}$ sec. It is found that this time is much

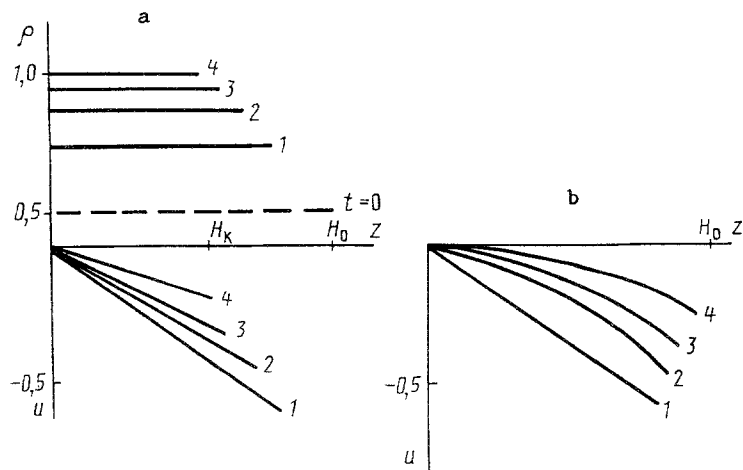


Fig. 1. (a) Distribution of the density ρ along the pressing height at different times of the process: 1) $\tau = 10^{-3}$ sec; 2) $5 \cdot 10^{-3}$; 3) 10^{-2} ; 4) 0.5; (b) trends in the formation of the linear profile of velocity u (m/sec) in the regular mode of compaction: 1) $\tau = 10^{-3}$ sec; 2) 10^{-4} ; 3) 10^{-5} sec; 4) 10^{-6} ; parameters: $H_0 = 0.1$ m, $N_p = 10^9$ Pa, and $\eta_1 = 10^6$ Pa·sec.

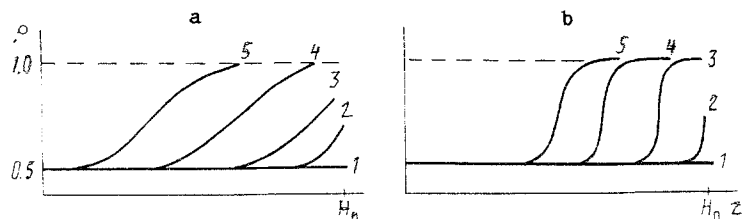


Fig. 2. Distribution of the density ρ along the pressing height: 1) $\tau = 0$; 2) $1.3 \cdot 10^{-5}$ sec; 3) $3 \cdot 10^{-5}$; 4) $7 \cdot 10^{-5}$; 5) $9 \cdot 10^{-5}$; calculation parameters: $H_0 = 0.1$ m; $\rho_1 = 5 \cdot 10^3$ kg/m³; (a) $\eta_1 = 10^5$ Pa·sec; $N_p = 10^9$ Pa; (b) 10^5 and 10^{12} .

shorter than the characteristic compaction time, which can be estimated for the chosen parameters: $\tau_* = 4\eta_1/3N_p = 10^{-3}$ sec. Thus, if the material is compacted under the manifestly evident regular mode operation, the system does not experience the inertial factor, since inertia manifests itself during the very short initial time of the process. The analytic solution of the problem, obtained by neglecting the inertia of the medium [3], can be used for investigating the compaction process in the Re_x range.

The other limiting case — compaction of a hot, porous billet under wave conditions — occurs in the range of Re values starting with a certain lower limit, $Re_{**} \sim 25$ (Fig. 2a). If $Re \gg Re_{**}$ (for instance, $Re \sim 50-70$), the compaction wave has a narrow front (Fig. 2b). In the process of analyzing numerically the model of the wave compaction mode, one can find the transient time τ_{tr} of establishment of the operating mode resulting from the unsteadiness of the process. It is determined by the magnitude of the wave formation segment and the wave propagation velocity throughout the volume of the material to be compacted. For instance, for $\eta_1 = 10^5$ Pa·sec, $N_p = 10^{11}$ Pa, $H_0 = 0.1$ m, $\rho_0 = 0.5$, $\rho_1 = 5 \cdot 10^3$ kg/m³, transition to the wave mode occurs during the time $\tau_{tr} = 10^{-7}$ sec.

However, another factor must be taken into account besides the characteristic compaction time τ_* : the pressing time τ_p . This is an extraneous parameter and is considered to be assigned. For the wave mode of operation to develop in compaction, it is necessary that

$$\tau_{tr} \ll \tau_* < \tau_p \quad (9)$$

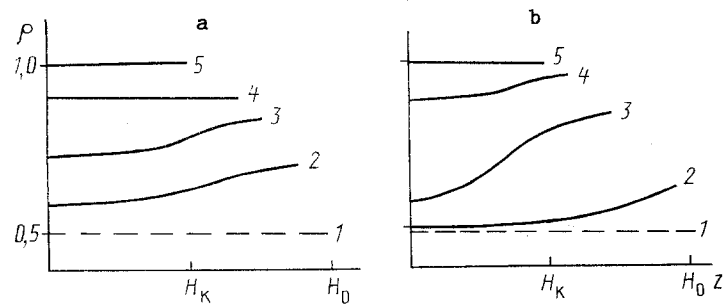


Fig. 3. Distribution of the density ρ along the pressing height $H_0 = 0.1$ m at different process times: 1) $\tau = 0$; 2) $6.5 \cdot 10^{-6}$ sec; 3) $1.5 \cdot 10^{-5}$ sec; 4) 10^{-4} sec; 5) 10^{-3} sec; parameters: a) $\eta_1 = 10^6$ Pa·sec; $N_p = 10^{10}$ Pa; b) 10^5 and 10^{10} .

It is clear that, if one of the inequalities in (9) is not satisfied, either uncompacted regions remain in the material or the compaction wave cannot form at the end of the force application time in the press. It should be noted that numerical calculations support the validity of the asymptotic behavior for the above range of Reynolds numbers that has been suggested in [4].

The values of the Reynolds number lying between the limiting values Re_* and Re_{**} correspond to transient compaction conditions. These conditions (Fig. 3) combine the properties of both wave and regular operating modes, which, however, manifest themselves to a greater or lesser degree, depending on the specific Re value. If Re is close to Re_* , the characteristics of the transient mode are closer to those of the regular mode. However, there is a significant feature: There is no self-equalization of the density from the very beginning of the process, which is characteristic for the regular mode of compaction. One can say even more: If the initial density throughout the volume of the material is the same (there is no density variation) a density gradient develops under this set of transient conditions. This characteristic obtains during hydrodynamic stabilization, after which the usual pattern occurs, and the material is compacted under the regular operating mode.

If $Re \rightarrow Re_{**}$, the transient operating mode is closer to the wave mode, with the difference, however, that the front of the compaction wave is broad and blurred, not narrow as in the case of $Re > Re_{**}$. For transient compaction conditions, the time during which the system reaches a steady state is important and must not be neglected. This means that studies of the compaction processes characterized by $Re_* < Re < Re_{**}$ reach beyond the framework of approximate models, where transient processes are neglected, and can be carried out only on the basis of numerical considerations of a generalized model.

NOTATION

t and x , time and present height, respectively (Euler coordinates); τ and q , time and present mass, respectively (Lagrange coordinates); ρ , density of the material relative to the density of its incompressible base ρ_1 ; u and σ , components of the velocity and stress tensors in the longitudinal direction, respectively; η_1 , viscosity of the incompressible base; N_p and u_p , force acting in the press and plunger velocity, respectively; H_0 and M , initial pressing height and mass, respectively; ρ_0 , initial pressing density.

LITERATURE CITED

1. L. M. Buchatskii, A. M. Stolin, and S. I. Khudyaev, *Poroshk. Metall.*, No. 9, 37-41 (1986).
2. L. M. Buchatskii, A. M. Stolin, and S. I. Khudyaev, *Poroshk. Metall.*, No. 12, 9-14 (1987).
3. A. M. Stolin, N. N. Zhilyaeva, and B. M. Khusid, *Inzh.-Fiz. Zh.*, 59, No. 2, 248-254 (1990).
4. N. N. Zhilyaeva and A. M. Stolin, *Inzh.-Fiz. Zh.*, 59, No. 6, 984-988 (1990).
5. L. S. Stel'makh, N. N. Zhilyaeva, and A. M. Stolin, "Non-isothermic Rheodynamics in Superhigh-Speed Pressing of Powder Materials," Preprint, Institute of Metallurgy, Academy of Sciences of the USSR, Chernogolovka (1990).